

Supporting Information for

Unusual nanosized associates of carboxy-calix[4]resorcinarene and cetylpyridinium chloride: the macrocycle as a glue for surfactant micelles

Ju. E. Morozova,^{a,b} V. V. Syakaev,^a Ya. V. Shalaeva,^{a,b} A. M. Ermakova,^{a,b} I. R. Nizameev,^{a,c} M. K. Kadirov,^a I. S. Antipin,^{a,b} A. D. Voloshina,^a V. V. Zobov^a and A. I. Konovalov^a

^aA. E. Arbuzov Institute of Organic and Physical Chemistry, Kazan Scientific Center, Russian Academy of Science, Arbuzov str. 8, 420088 Kazan, Russian Federation

^bKazan Federal University, Kremlevskaya st. 18, 420008 Kazan, Russian Federation

^cKazan National Research Technical University, K. Marx str. 10, 420111 Kazan, Russian Federation

Table of Contents

	page
Figure S1. The percentage hemolysis of human red blood cells in the distilled water (H_2O), in 0.15 M NaCl solution (control), and in the solution of CR (0.5 mM) in 0.15 M NaCl (CR 0.5 mM).	3
Table S1. The CR/CPC solutions for DLS	3
Figure S2. ^1H NMR spectra of CPC and CR·8CPC in CDCl_3 (5 mM).	4
Table S2. The values of averaged hydrodynamic diameters of particles (d, nm), their intensities of scattering (%) and polydispersity index (PDI) in mixed solutions of CR - CPC (25 °C, DLS data).	5
Figure S3. ^1H NMR spectra of the solutions in D_2O of CR (1 mM), CR/CPC 1/1 (C(CPC) = 1 mM), CR/CPC 1/4 (C(CPC) = 2 mM), and CPC (1 mM).	6
Table S3. The data of ^1H NMR spectrum of CPC and C5Pyr, and their $\Delta\delta$ (ppm) in solutions with CR in D_2O .	7
The study of fluorescence anisotropy of DPH in CR-CPC solutions	
Figure S4. Fluorescence anisotropy of DPH in CPC-CR solutions (C(CR) = 1 mM) at 25 °C.	8
Figure S5. The Job's curves for CR-C5Pyr solutions (^1H NMR data) (a) and the proposed structure of CR·2 C5Pyr complex (MM2 force field, ChemBioDraw Ultra 11.0) (b).	9
Table S4. The NMR FT-PGSE data for CR, C5Pyr and CR-C5Pyr solutions in D_2O .	9
Table S5. The values of averaged hydrodynamic diameters of particles (d, nm), their intensities of scattering (%) and polydispersity index (PDI) for CR-CPC (1/1, 1 mM) solution in the conditions of heating from 25°C to 60°C and subsequent cooling to 25	

°C (DLS data).	10
Table S6. The values of averaged hydrodynamic diameters of particles (d, nm), their intensities of scattering (%) and polydispersity index (PDI) for CR-CPC (1/1) solutions of different concentration obtained by dilution (25 °C, DLS data).	10
The <i>cca</i> values study of CR-CPC (1/1) and CPC in 0.15 M NaCl and PB (pH 7.4)	10
Figure S6. The dependence of I/III values of pyrene on concentration of CPC (a) and SNPs (b) in the presence of 0.15 M NaCl and PB (pH 7.4).	
Table S7. The values of averaged hydrodynamic diameters of particles (d, nm), their intensities of scattering (%) and polydispersity index (PDI) of SNPs (CR/CPC 1/1, 0.078 mM) in PB solutions (25 °C, DLS method).	11
The complex stability constant of R6G with CR and SNPs.	
Figure S7. a - The dependence of the differential fluorescence intensity of R6G (C = 0.038 mM) on the concentration of quencher Q (CR or SNPs). b - Stern-Volmer plot for R6G quenching by CR and SNPs.	11
Figure S8. The proposed scheme of the R6G and MY binding by SNPs.	12
References	12

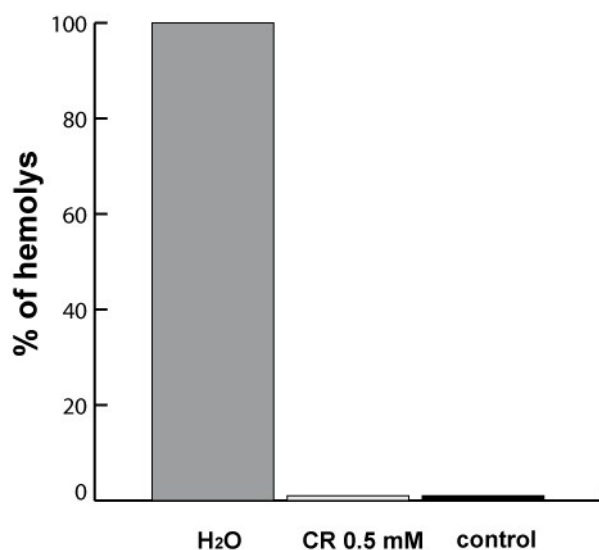


Figure S1. The percentage hemolysis of human red blood cells in the distilled water (H₂O), in 0.15 M NaCl solution (control), and in the solution of CR (0.5 mM) in 0.15 M NaCl (CR 0.5 mM).

Table S1. The CR/CPC solutions for DLS

NN	C(CPC)/C(CR)	C(CPC), mM	C(CR), mM	the kind of solution
1	30/1	0.997	0.033	O ^[a]
2	25/1	0.996	0.040	O
3	20/1	0.995	0.050	O
4	16/1	0.994	0.062	O
5	14/1	0.993	0.071	O
6	12/1	0.992	0.083	O
7	10/1	0.990	0.099	O
8	8/1	0.988	0.123	P ^[b]
9	4/1	0.976	0.244	O
10	2/1	0.952	0.476	O
11	1/1	0.909	0.909	O
12	1/2	0.833	1.670	O
13	1/4	0.714	2.860	O
14	1/8	0.556	4.440	O
15	1/10	1.000	10.00	O
16	1/15	1.000	15.00	T
17	1/20	2.000	20.00	T

[a] O – opalescence, [b] P – precipitation, [c] T - transparence

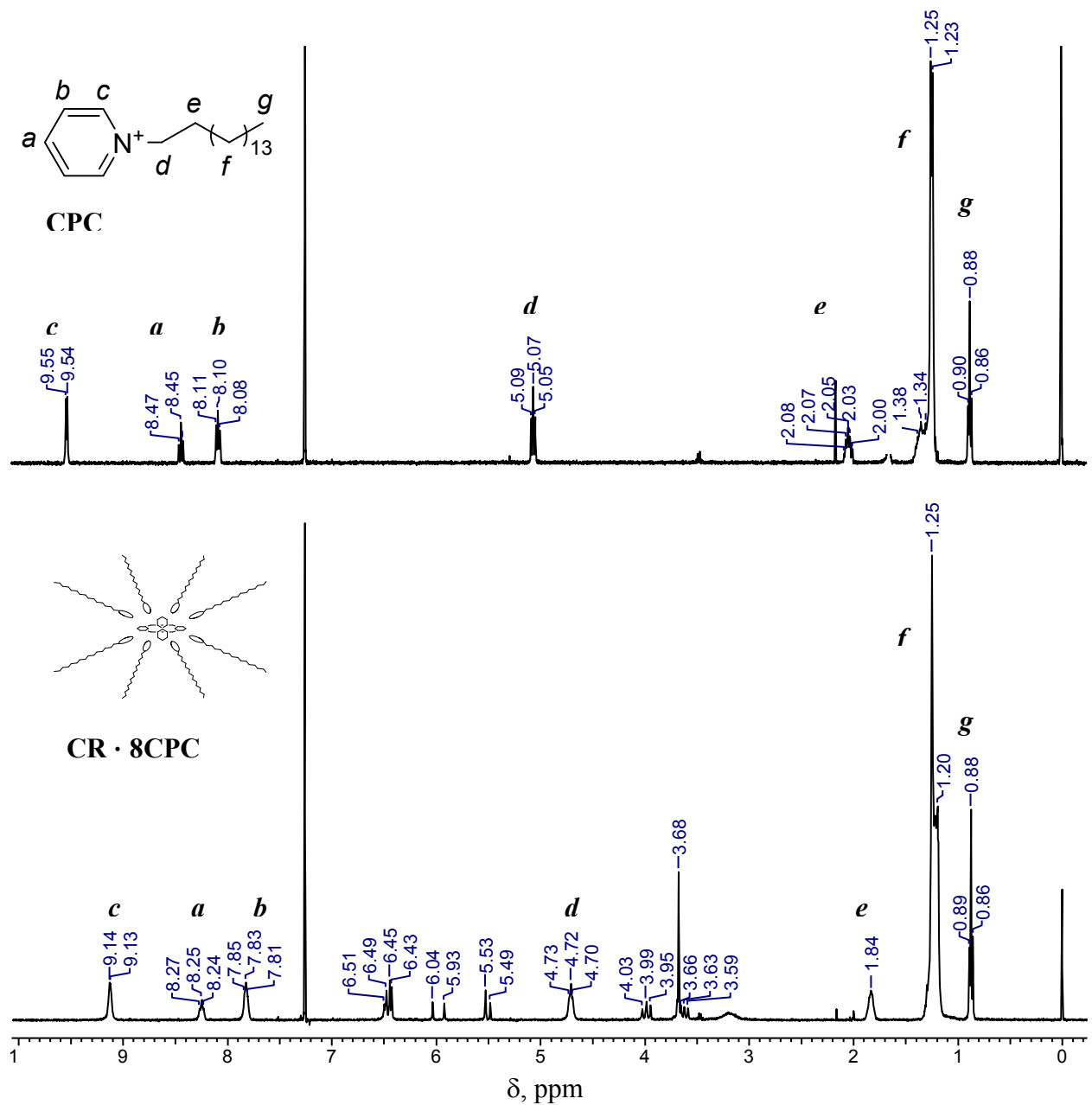


Figure S2. ^1H NMR spectra of CPC and CR · 8CPC in CDCl_3 (5 mM).

The large shifts of proton signal of pyridinium fragment and N^+CH_2 group of CPC in associate with CR are observed that indicate the proximity of pyridinium group of CPC molecules to the aromatic rings of CR and the formation of hydrophobic complex.

Table S2. The values of averaged hydrodynamic diameters of particles (d, nm), their intensities of scattering (%) and polydispersity index (PDI) in mixed solutions of **CR - CPC** (25 °C, DLS data).

C(CPC)/ C(CR)	fresh		after 14 d		after 28 d		after 35 d	
	d, nm (I, %)	PDI	d, nm (I, %)	PDI	d, nm (I, %)	PDI	d, nm (I, %)	PDI
30/1	91 (15)	0.14	79 (27)	0.104	n/c ^[b]	0.457	-	-
25/1	106 (12)	0.19	91 (24)	0.085	n/c	0.612	-	-
20/1	79 (12)	0.169	91 (22)	0.086	n/c	0.703	-	-
16/1	91 (13)	0.143	106 (43)	0.038	79 (59)	0.14	n/c	1.0
14/1	91 (15)	0.134	91 (26)	0.092	91 (30)	0.031	91 (30) ^[c]	0.184
12/1	106 (14)	0.151	91 (13)	0.161	n/c	0.088	-	-
10/1	164 (19)	0.137	91 (21)	0.126	n/c	-	-	-
8/1	P ^[a]	-	-	-	-	-	-	-
4/1	164 (28)	0.04	190 (43)	0.005	220 (16)	0.157	n/c	0.571
2/1	164 (28)	0.069	164 (24), 615 (0.5)	0.234	n/c	0.978	-	-
1/1	164 (22)	0.067	220 (19), 825 (4)	0.217	255 (33)	0.095	255 (54) ^[c]	0.049
1/2	122 (7), 295 (12)	0.233	190 (25)	0.12	295 (42)	0.156	n/c	1.0
1/4	164 (23)	0.071	220 (41)	0.02	295 (43)	0.257	190 (4), 531 (16) ^[c]	0.195
1/8	164 (25)	0.039	295 (52)	0.012	n/c	0.831	-	-
1/10	164 (28)	0.039	n/c	0.451	-	-	-	-
1/15	n/c	0.817	-	-	-	-	-	-
1/20	n/c	0.418	-	-	-	-	-	-

[a] P – precipitation; [b] n/c - exponential particle size–population curve is not correct; after 42 days – n/c.

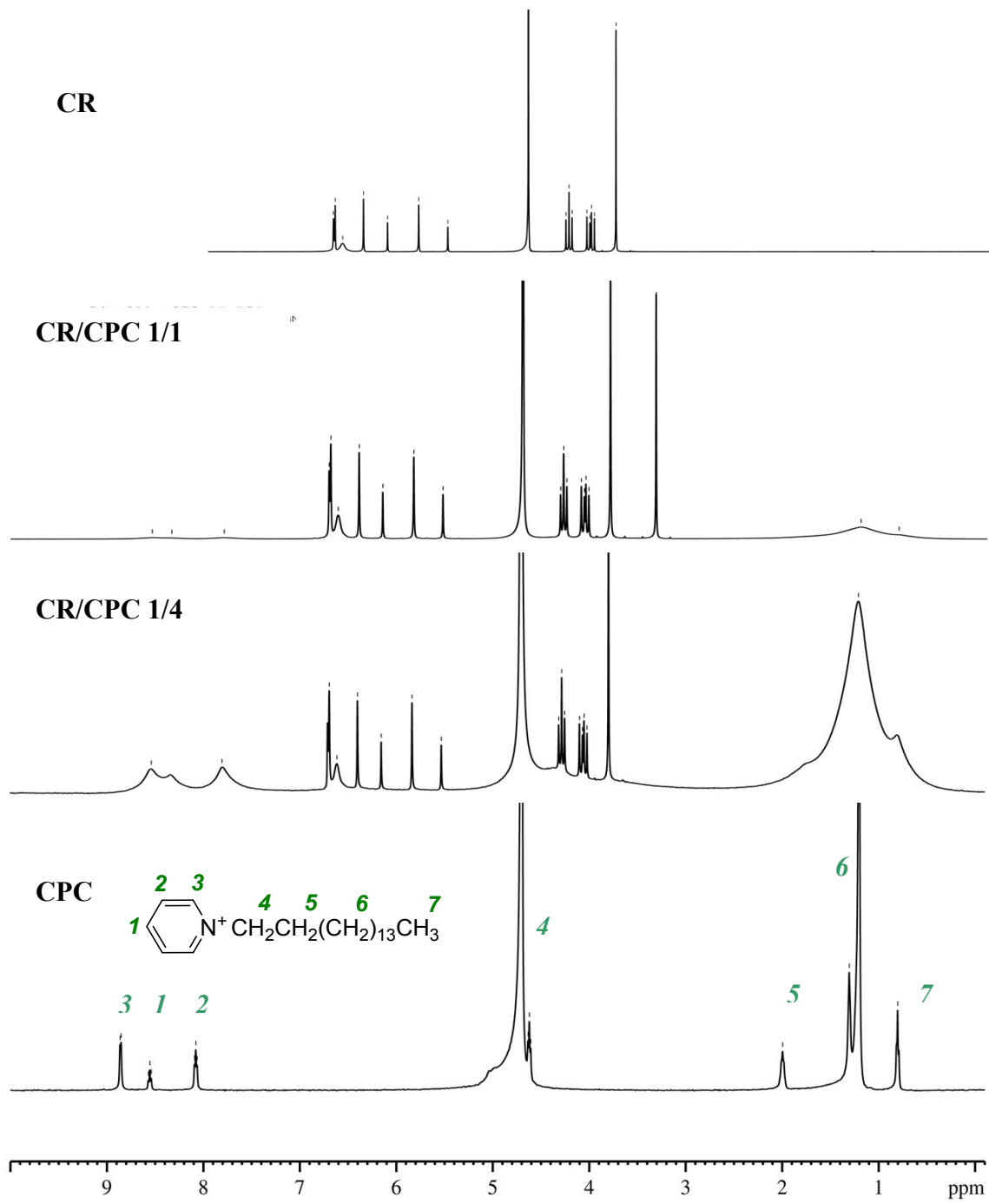
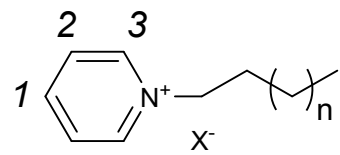


Figure S3. ¹H NMR spectra of the solutions in D₂O of CR (1 mM), CR/CPC 1/1 (C(CPC) = 1 mM), CR/CPC 1/4 (C(CPC) = 2 mM), and CPC (1 mM).

Table S3. The data of ¹H NMR spectrum of CPC and C5Pyr, and their $\Delta\delta$ (ppm) in solutions with CR in D₂O.



CPC $X^- = Cl^-$ $n = 12$

C5Pyr $X^- = Br^-$ $n = 2$

	δ , ppm	$\Delta\delta$, ppm			δ , ppm	$\Delta\delta$, ppm
		CPC	CPC/CR 1/4	CPC/CR 1/1		
C(CPC), mM	1.25	2		1	1.25	5
C(CR), mM	-	0.5		1	5	-
ArH1	8.56	-0.01		-0.03	-0.23	8.51
ArH2	8.08	-0.26		-0.27	-0.28	8.03
ArH3	8.86	-0.52		-0.52	-0.31	8.80
N^+CH_2	4.62	ov ^[a]		ov	ov	4.57
$N^+CH_2CH_2$	2.00	br ^[b]		br	-0.27	1.98
$N^+CH_2CH_2(CH_2)_n$	1.20	0.02		0.02	0.02	1.34-1.26
$N^+CH_2CH_2(CH_2)_nCH_3$	0.80	br		br	0.01	0.83

[a] ov – overlapping signal; [b] br – broadening signal

The study of fluorescence anisotropy of DPH in CR-CPC solutions

The morphology of association can be studied by using of fluorescent probe 1,6-diphenyl-1,3,5-hexatriene (DPH, Sigma), which can include into the hydrophobic parts of associates and react to the changes of microenvironment's anisotropy [1]. Steady-state fluorescence anisotropy of DPH was measured at 25 °C on a Cary Eclipse (USA) spectrometer equipped with filter polarizers. DPH were excited at 361 nm, and the fluorescence intensity was measured at 467 nm. The excitation and emission slit widths were 5 nm. A quartz cell of 1 cm path length was used for all fluorescence measurements. The concentration of fluorescence probe DPH of 0.05 mM was used. CPC solutions were prepared by the stepwise dilution of a CPC-CR solution (1 mM, CR/CPC 1/1) by 1 mM solution of CR, the concentration of CPC varied from 1 mM to 0.01 mM. The embedded software automatically determined the correction factor and anisotropy value.

Figure S4 shows the concentration dependence of the anisotropy for the CPC in the presence of 1 mM CR. It's expected that changing of the anisotropy should be observed closer to cca value (about 0.1 mM CPC). As can be seen, the same r values are observed in all investigated solutions (**Figure S4**). Since all studied solutions contain the 1 mM CR it should be assumed that the DPH is bound by macrocycle and is not involved in the CPC micellization. The same bonding of DPH by macrocycle is observed in the solutions of viologen-resorcin[4]arene cavitand [2]. So, unfortunately, the confirmation of the morphology of the CPC-CR solutions is failed because of the formation of the complex DPH-CR.

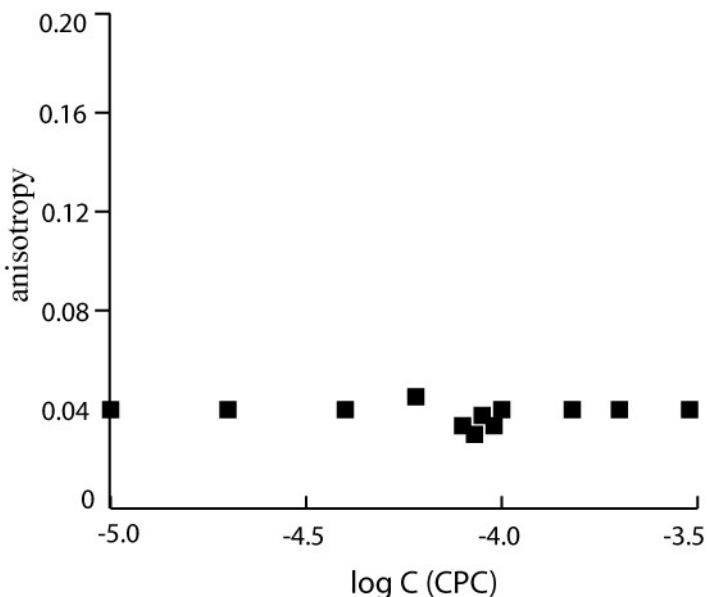


Figure S4. Fluorescence anisotropy of DPH in CPC-CR solutions ($C(CR) = 1$ mM) at 25 °C.

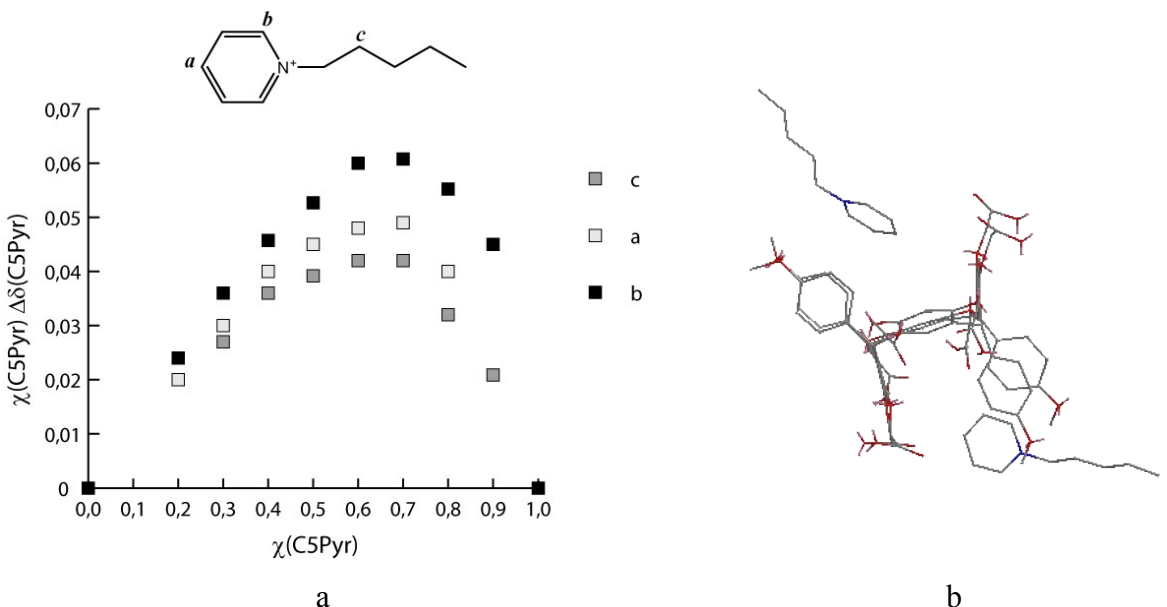


Figure S5. The Job's plot for CR- C5Pyr solutions (^1H NMR data) (a) and the proposed structure of CR-2 C5Pyr complex (MM2 force field, ChemBioDraw Ultra 11.0) (b).

The stoichiometry of CR-C5Pyr complexation has been determined by the continuous variation (Job) method [3], where the overall concentration of components in the solution are constant (5 mM), and their mole fractions (χ) vary from 0 to 1. The maximum in the Job curve is 0.67 that indicates the 1:2 complex formation in the solution (Figure S5a).

The pyridinium fragment of guest is located near to aromatic units of substituents of CR. The molecule of CR is in the chair conformation; two guest molecules are located on either side of the plane in which the both opposite macrocycle rings are situated (Figure S5b).

Table S4. The NMR FT-PGSE data for CR, C5Pyr and CR-C5Pyr solutions in D_2O : D_s - self-diffusion coefficient, R_H^{exp} and R_H^{teor} - experimental and theoretical value of hydrodynamic radii of CR, N_{ag} - the aggregation number, P_{bD} – the fraction of bound C5Pyr.

	$C, \text{ mM}$		$D_s (\times 10^{-10} \text{ m}^2/\text{s})$		$R_H (\text{\AA})$		CR	N_{ag}	P_{bD}
	CR	C5Pyr	CR	C5Pyr	exp	teor ^c			
CR	5	-	2.51	-	11	8.7	2.0	-	-
C5Pyr	-	5	-	8.02	-	-	-	-	-
CR + C5Pyr	5	1.25	2.47	6.12	11.3	-	2.2	0.34	

The fraction of bound guest (P_{bD}) in two-site model for the case of the fast exchange between bound and unbound states of a guest molecule in the NMR time scale was calculated as described in [4] $P_{bD} = (D_{\text{obs}} - D_{\text{free}})/(D_{\text{comp}} - D_{\text{free}})$, where D_{obs} is the apparent (weighed average) self-diffusion coefficient of the guest molecule in the complex, D_{comp} is the self-diffusion coefficient of the complex and D_{free} is the self-diffusion coefficient of the free guest in the same solvent. D_{comp} is assumed equal to D_{host} – the self-diffusion coefficient of the macrocycle.

Table S5. The values of averaged hydrodynamic diameters of particles (d, nm), their intensities of scattering (%) and polydispersity index (PDI) for CR-CPC (1/1, 1 mM) solution in the conditions of heating from 25°C to 60°C and subsequent cooling to 25 °C (DLS data).

t, °C	d, nm	I, %	PDI
25	164.2 (50.75-342)	19.8	0.092
35	164.2 (58.77-342)	23.8	0.082
40	164.2 (105.7-712.4)	22.2	0.093
50	164.2 (105.7-342)	24.5	0.103
60	190.1 (105.7-342)	22.4	0.097
25	190.1 (141.8-255)	33.4	0.060

Table S6. The values of averaged hydrodynamic diameters of particles (d, nm), their intensities of scattering (%) and polydispersity index (PDI) for CR-CPC (1/1) solutions of different concentration obtained by dilution (25 °C, DLS data).

C(CR), mM	C(CPC), mM	d, nm	I, %	PDI
0.909	0.909	164.2 (50.75-295.3)	22.5	0.067
0.0909	0.0909	164.2 (91.28-295.3)	22.8	0.056
0.00909	0.00909	164.2 (105.7-295.3)	25.6	0.084

The cca values study of CR-CPC (1/1) and CPC in 0.15 M NaCl and PB (pH 7.4)

As known, the hydrophobic interactions in the surfactant's micelles in the presence of electrolytes are intensified that lead to the decrease of its critical micelle concentration (*cmc*). In the presence of 0.15 M NaCl and PB (pH 7.4) *cmc*-values of CPC of 0.21 mM and 0.215 mM, respectively, were obtained (pyrene fluorescence, **Figure S6**). In the same conditions the enhancement of hydrophobic interactions in the CR-CPC associates (SNPs) leads to the limitation of it's solubility above 0.1 mM, and the correct sigmoidal plots I/III($\log C(\text{SNPs})$) can not be obtained (**Figure S6**). In the presence of 0.15 M NaCl and PB the SNPs exist from 0.03 to 0.1 mM.

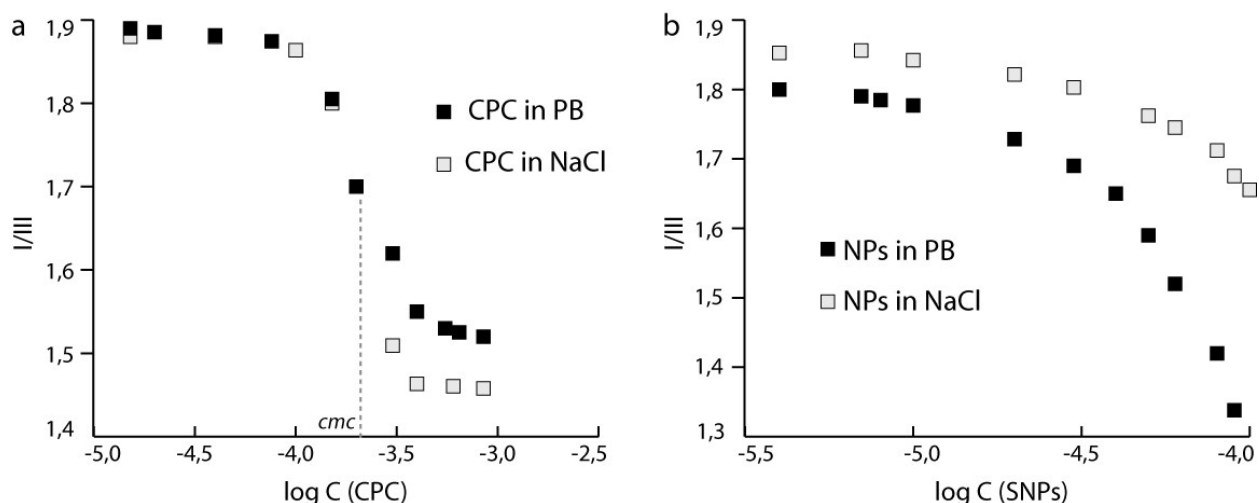


Figure S6. The dependence of I/III values of pyrene on concentration of CPC (a) and SNPs (b) in the presence of 0.15 M NaCl and PB (pH 7.4).

Table S7. The values of averaged hydrodynamic diameters of particles (d, nm), their intensities of scattering (%) and polydispersity index (PDI) of SNPs (CR/CPC 1/1, 0.078 mM) in PB solutions (25 °C, DLS method).

	d, nm (I, %)	PDI
pH 8	142 (18)	0.130
pH 7.08	142 (16)	0.123
pH 6.07	142 (22)	0.144
pH 5	164 (17)	0.167
pH 3.98	190 (26)	0.046
pH 3.05	n/c ^[a] , P ^[b]	0.444
pH 2.12	n/c, P	1.000

[a] n/c - exponential particle size–population curve is not correct; [b] P – precipitation after 24 h.

The complex stability constant of R6G with CR and SNPs.

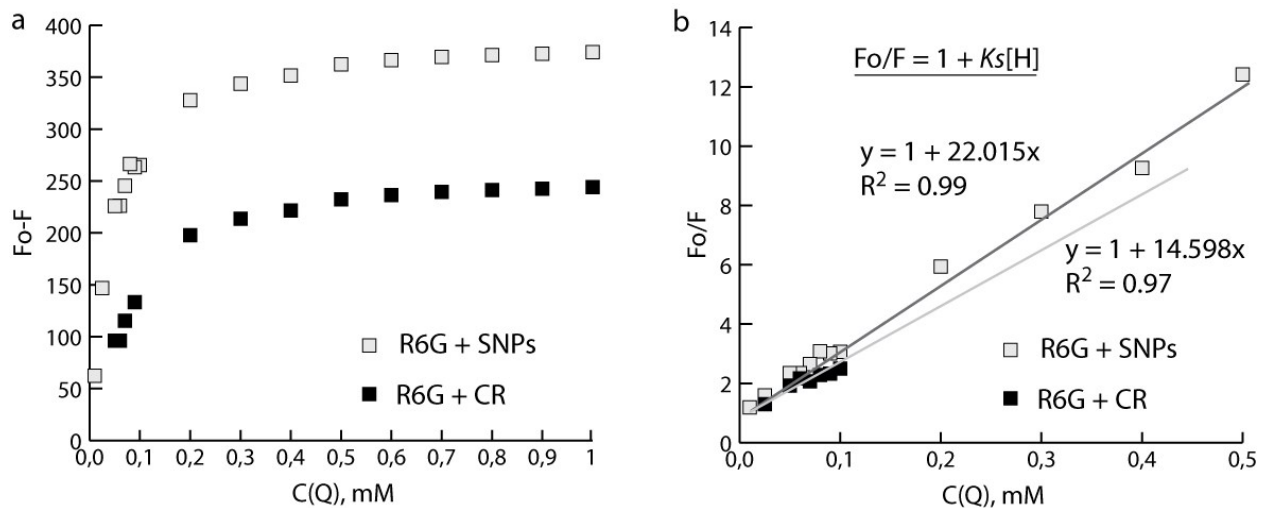


Figure S7. a - The dependence of the differential fluorescence intensity of R6G ($C = 0.038$ mM) on the concentration of quencher Q (CR or SNPs). b - Stern-Volmer plot for R6G quenching by CR and SNPs.

The fluorimetry titration of R6G by molar ratio method in the presence of CR or SNPs (CPC/CR 1/1) showed the exponential decrease in the intensity of dye with the increasing of the concentration of quencher (Figure S7a). According to the Stern-Volmer equation $F_0/F = 1 + K_s[Q]$, where F_0 and F - are the fluorescence of fluorophore in the absence and in the presence of quencher, respectively, K_s - the constant of static quenching (complex stability constant), $[Q]$ - concentration of the quencher) [1]. The slope of $F_0/F([Q])$ slope give the value of K_s (Figure 7b). The values of association constant are 15000 and 22000 M⁻¹ for R6G-CR and R6G-SNPs, respectively.

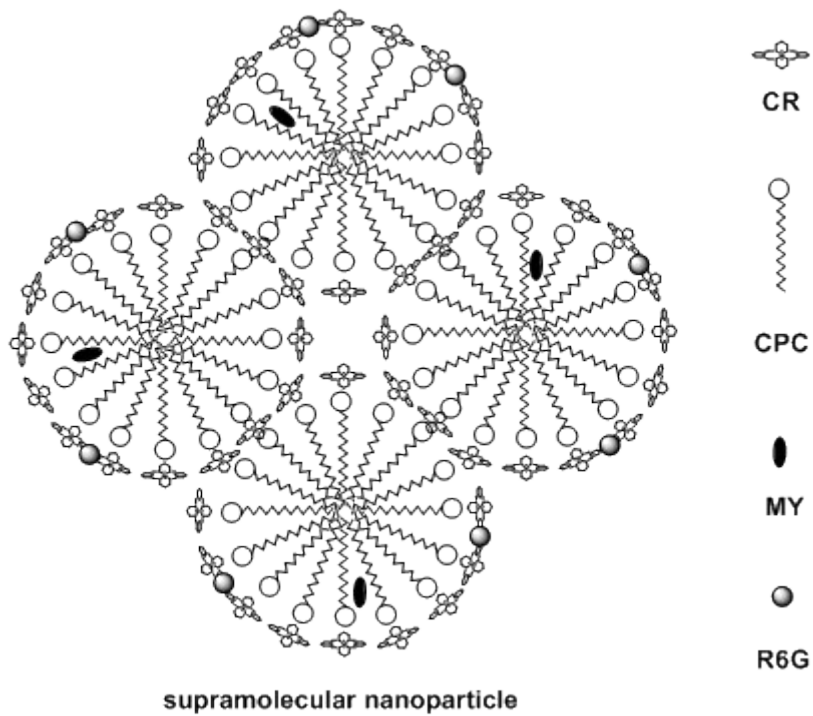


Figure S7. The proposed scheme of the R6G and MY binding by SNPs.

References

1. J. R. Lakowicz, *Principles of Fluorescence Spectroscopy*, Springer, 3rd edition, 1986.
2. R. R. Kashapov, S. V. Kharlamov, E. D. Sultanova, R. K. Mukhitova, Yu. R. Kudryashova, L. Y. Zakharova, A. Y. Ziganshina, A. I. Konovalov. *Chem. Eur. J.*, 2014, 20, 14018 – 14025.
3. K. Hirose, *J. Incl. Phenom. Macro.*, 2001, 39, 193-209.
4. V. V. Syakaev, E. Kh. Kazakova, Ju. E. Morozova, Ya. V. Shalaeva, Sh. K. Latypov and A. I. Konovalov, *J. Colloid Interface Sci.*, 2012, 370, 19-26.